*SECTION 3*

## PHYSICS OF RADIATION AND ION-PLASMA TECHNOLOGIES

*https://doi.org/10.46813/2025-159-103*

UDC 621.793:539.21

# EFFECT OF COMPOSITION AND STRUCTURE ON PROTECTIVE PROPERTIES OF Ti-Cr-N VACUUM ARC COATINGS

***Yu.A. Zadneprovskiy[1], V.A. Bilous[1], E.N. Reshetnyak[1], V.S. Goltvyanytsya[2]***
***[1]National Science Center "Kharkiv Institute of Physics and Technology", Kharkiv, Ukraine;***
***[2]National University "Zaporizhzhia Polytechnic", Zaporizhzhia, Ukraine***
***E-mail: yaz@kipt.kharkov.ua***

In this work, we investigated the cavitation, abrasion and corrosion resistance of vacuum arc coatings Ti-Cr-N. Nanostructured coatings with a thickness of 10 μm were deposited on AISI 430 steel substrates from filtered plasma flow using Ti-Cr cathodes containing 23 and 32 wt.% Cr at nitrogen pressure from 0.12 to 0.67 Pa. Nanocrystalline (nc) or amorphous-nanocrystalline (a/nc) coatings based on cubic solid solution $(Ti_{1-x},Cr_x)N$ with chromium content from x = 0.11 to x = 0.25, CSZ size in the range of 6…14 nm and different axial textures were tested. The coatings had a high hardness of 31…46 GPa, however, changes in the cathode composition and/or nitrogen pressure during deposition affected the chromium content in the coatings and their structure, which altered their protective properties. Nevertheless, all the studied coatings effectively protected the steel substrate during testing. Nc coatings with a low Cr content of 11…13 at.% and a hardness of 30…33 GPa shown the best cavitation wear resistance. The reduction in the crystallites size of the solid solution $(Ti_{1-x},Cr_x)N$ and the formation of the [110] texture contributed to the improvement of cavitation resistance. Coatings with a high Cr content of 18…24 at.% had the best abrasion resistance, besides the a/nc structure with a high hardness of about 46 GPa had certain advantages, but it showed the worst results in cavitation and corrosion tests. The nc$(Ti_{0.87}Cr_{0.13})N$ coating with a [111] texture and a hardness of 33 GPa proved to be the most corrosion-resistant, although it had the worst resistance to abrasive wear. The appearance of the anodic polarisation curve for this coating differs from other specimens and has a secondary passivated region. It has been shown that optimizing the deposition parameters during the synthesis of coatings with a high Cr content of about 25 at.% allows for further improvement of the abrasive or corrosion resistance of coatings with a/nc and nc structures, respectively. With regard to the comprehensive protection of steel products from cavitation, abrasion and corrosion, the use of nanocrystalline coatings appears to be the most appropriate.

## INTRODUCTION

Modern energy equipment operates under harsh conditions of abrasive wear, cavitation, and aggressive environments [1]. During the long-term operation of power equipment, changes in loads, temperatures, and hydrogen-containing media cause the structural, phase, and physical properties of the steel in this equipment to change, especially in the hydrogen-cooled turbogenerator [2]. The working blades of the last stages of the low-pressure cylinders of high-power steam turbines are also susceptible to wear damage [3]. For instance, cavitation can damage steels of various structural types (austenitic and ferritic-martensitic) [4] as well as alloyed titanium alloys [5, 6]. Material wear can lead to a significant damage and equipment failure [7].

Due to the increasing maintenance costs associated with cavitation erosion and/or erosion caused by solid particles in hydraulic machines and tribological connections, protecting the surfaces of these components is crucial [8]. The use of ion-plasma coatings based on titanium nitride [9] or complex alloy coatings [10, 11] can significantly reduce surface wear of materials, thereby increasing the reliability and service life of equipment. Testing materials and coatings for cavitation wear allows predicting their stability and protective properties under operating conditions [12].

A modern method for obtaining hard nanostructured coatings is vacuum arc deposition using multicomponent cathodes [13, 14]. Vacuum arc coatings based on transition metal nitrides using Cr as an alloying element are characterized by increased mechanical, corrosion, and erosion resistance, as well as resistance to oxidation at high temperatures, and can be used to protect nuclear reactor fuel elements [15]. Despite the wide variety of work in this area [16–21], the question of the influence of the structure of Ti-Cr-N coatings on their operational characteristics when using Ti-Cr cathodes in a wide range of Cr additives is of interest. To a large extent, it can depend on the deposition conditions: in a direct or filtered plasma flow. A known advantage of deposition in a separated flow is the production of homogeneous coatings that do not contain macroparticles; a disadvantage is the low deposition rates. Deposition from a filtered flow allows protective coatings coating of various compositions with higher performance characteristics to be obtained. However, publications on this topic pay little attention to the Ti-Cr-N coatings [22, 23]. Coatings for energy equipment must provide effective protection of the part working surface from combination of destructive factors, the main ones being cavitation, abrasive wear, and corrosion. The protective characteristics of coatings are determined by their composition and structure [9, 10, 24].

In our recent work [25], we investigated the elemental composition, structure, and mechanical properties of Ti-Cr-N coatings deposited in a wide range of nitrogen pressures from unfiltered and filtered vacuum arc plasma flows from Ti-Cr alloy cathodes containing 23 and 32 wt.% chromium. It was shown that the use of a filter allows the droplet component to be effectively separated from the plasma flow and coatings with reduced surface roughness to be obtained. Coatings obtained from filtered plasma in the nitrogen pressure range of 0.12…0.67 Pa have a high hardness of 31…45 GPa due to the formation of a nanostructured cubic solid solution (Ti,Cr)N with an NaCl-type HSC structure. However, changes in the cathode composition and/or nitrogen pressure during deposition affect the chromium content in the coatings and their substructure, which can alter their protective properties. Studying the wear resistance of such coatings under various influences is interesting for understanding both physical processes and practical applications. The aim of this work was to test nanostructured vacuum arc Ti-Cr-N coatings for cavitation, abrasive wear resistance and corrosion in a 3 wt.% NaCl solution. The influence of chromium content and coating structure on their protective characteristics was analysed.

## EXPERIMENTAL DETAIL

Vacuum arc Ti-Cr-N coatings were deposited on a Bulat-type installation using plasma sources with magnetic cathode spot retention and plasma flow focusing [26]. Vacuum arc remelting process was used for the production of two-component Ti-Cr cathodes: Ti-23wt.%Cr ($Ti_{0.78}Cr_{0.22}$) and Ti-32wt.%Cr ($Ti_{0.7}Cr_{0.3}$). A linear filter [27] with a Ø 60 mm was used to filter the plasma flow. This filter was located at a distance of 150 mm from the cathode surface. The cathode-substrate distance was 350 mm. Coatings with a thickness of about 10 μm were deposited on AISI 430 steel substrates with dimensions of 20×10×1.5 mm. The main deposition parameters were: arc current – 90 A, substrate negative bias voltage – 270 V, nitrogen pressure within the range of 0.12…0.67 Pa.

The morphology of cross sections and the elemental composition of coatings were studied by scanning electron microscopy (SEM) on a JSM 7000-1F microscope equipped with an attachment for X-ray energy dispersive microanalysis. The phase composition of the coatings, the size of the coherent scattering zone (CSZ) and the texture were controlled by X-ray diffraction (XRD) on a DRON-3 diffractometer. The main deposition parameters and structural characteristics of coatings of different compositions (specimens #1–4) selected for testing resistance to various types of influences are given in Table 1. The data show that the used deposition modes made it possible to obtain nanocrystalline (nc) or amorphous-nanocrystalline (a/nc) coatings based on a cubic solid solution $(Ti_{1-x},Cr_x)N$ with a chromium content ranging from x = 0.11 to x = 0.25, an CSZ size ranging from 6 to 14 nm, and different axial textures [25].

Table 1

Deposition parameters and structural characteristics of coatings $(Ti_{1-x},Cr_x)N$

| Specimen # | 1 | 2 | 3 | 4 |
|---|---|---|---|---|
| Cathode compositions | $Ti_{0.78}Cr_{0.22}$ | | $Ti_{0.70}Cr_{0.30}$ | |
| Nitrogen pressure, Pa | 0.12 | 0.67 | 0.12 | 0.67 |
| Coating composition | $nc(Ti_{0.89}Cr_{0.11})N$ | $nc(Ti_{0.87}Cr_{0.13})N$ | $a/nc(Ti_{0.82}Cr_{0.18})N$ | $nc(Ti_{0.76}Cr_{0.24})N$ |
| CSZ dimension, nm | 7 | 14 | 6 | 8 |
| Axial texture | [110] | [111] | [100] | [110]+[111] |

The microhardness of the coatings was measured using a PMT-3 microhardness tester at a load of 0.5 N. Surface roughness was measured using a profilometer, and coating thickness was measured using microinterferometer MII-4.

The following methods were used to conduct laboratory studies of the performance characteristics of the specimens. Cavitation wear of specimens with deposited coatings was carried out on a device [9], which was an ultrasonic generator providing vibrations at a frequency of 20 kHz. The vibrations occurring in the aqueous medium led to erosion of the coating surface. Their degree of destruction was determined by weight loss Δm depending on the exposure time t to cavitation.

The abrasive wear of the specimen surfaces was investigated on the ABI-1 laboratory setup. The setup includes an electric motor, a shaft with an abrasive disc, a specimen mounting system, and a load. Wear was carried out according to the plane-disc scheme. A disc made of rubberized material containing abrasive particles served as a counterbody for flat specimens with coatings. The speed of the disc surface in contact with the specimen plane was 4.4 m/s, and the load on the specimen was 2.2 N. The level of abrasive wear was determined by the weight loss Δm depending on the test time t.

To study the corrosion resistance of the specimens, a potentiometric test method was used, which was carried out in an electrochemical cell of a PI-50-1 potentiostat at room temperature in a 3% NaCl aqueous solution. Anodic polarization curves were analyzed.

## RESULTS AND DISCUSSION

Fig. 1 shows electron microscope images of cross sections of coatings #1-4 (see Table 1) obtained from filtered vacuum arc plasma using cathodes containing different amounts of chromium ($Ti_{0.78}Cr_{0.22}$ and $Ti_{0.7}Cr_{0.3}$) at two nitrogen pressures in the vacuum chamber (0.12 and 0.67 Pa). It can be seen that the coatings are uniform in thickness and consist of nanoscale structural elements. No droplets of cathode material are observed in the coating, which indicates high plasma filtration quality. Changing the deposition parameters affects the structure of the fractures. Coatings #1, 2, and 4, which according to X-ray

structural analysis data have a nanocrystalline structure based on a solid solution of nc($Ti_{1-x}$,$Cr_x$)N with a cubic structure of the NaCl type, consist of narrow columnar grains. The structure of the fractures is dense, has a step-like appearance and is similar to the coating of the transition region between zone T and zone 2 of the Anders structural diagram [28]. Columnar growth is interrupted and the columns do not extend all the way from the substrate to the surface. The average transverse size of the columns is in the range of 100…150 nm. This cross-sectional morphology is typical for nanostructured nitride coatings obtained from filtered vacuum arc plasma [29].

The greatest thickness and width of columns is found in coating #2 nc($Ti_{0.87}Cr_{0.13}$)N, which correlates with the maximum value of the solid solution's average CSZ size of 14 nm, and the smallest is found in coating #1 nc($Ti_{0.89}Cr_{0.11}$)N with an average CSZ size of 7 nm. Enlarged images of the fractures of specimens #2 and 4 show the layering of the columns, which can be associated with the presence of texture in the coatings. In specimen #2, an axial texture with an axis [111] in the direction normal to the surface was found, i.e., the predominant arrangement of the BCC crystal grains with densely packed (111) planes parallel to the coating surface. Thus, the fracture of the specimen for microscopy runs across the (111) planes with the maximum bond density, i.e., the least preferred path for destruction, which leads to the formation of a layered relief across the columnar nitride crystals. A double texture [110]+[111] was found in coating #4, so in addition to the transverse layers, layers located at an angle of 30…40 degrees are observed in part of the columnar crystals, which corresponds quite well to the angle between the texture axes of 35 degrees. The fracture of coating #3 differs significantly from other specimens and has a dense morphology in the form of small rounded particles, which is due to the formation of an amorphous-nanocrystalline structure a/nc($Ti_{0.82}Cr_{0.18}$)N with the presence of a significant amount of amorphous phase, which interrupts columnar growth.

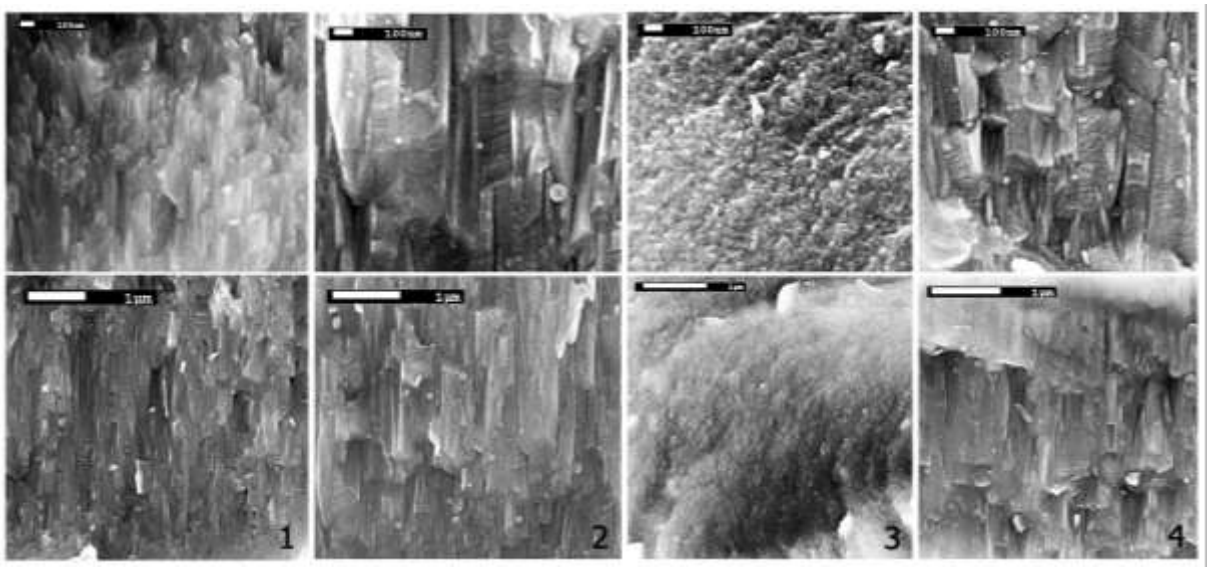


*Fig. 1. SEM images of a transverse fracture of the specimens #1–4 with coatings ($Ti_{1-x}$,$Cr_x$)N obtained using $Ti_{0.78}Cr_{0.22}$ (1, 2) and $Ti_{0.7}Cr_{0.3}$ (3, 4) cathodes at a nitrogen pressure in the vacuum chamber of 0.12 Pa (1, 3) and 0.67 Pa (2, 4). The images in the upper and lower rows differ in scale*

The results of electron microscopy do not show clear correlations between the elemental composition and morphology of the coatings. For example, coatings #2 nc($Ti_{0.87}Cr_{0.13}$)N and #4 nc($Ti_{0.76}Cr_{0.24}$)N, which differ twice in chromium content, have a similar nanocrystalline structure. Fig. 2,a shows the effect of cathode composition and changes in nitrogen pressure in the vacuum chamber during deposition on the chromium content in the coatings. It should be noted that with such changes in the deposition parameters, the nitrogen content in the coatings remains unchanged within the margin of error. As can be seen in Fig. 2,a, with an increase in nitrogen pressure from 0.12 to 0.67 Pa, an enrichment of the coatings with chromium is observed. For ($Ti_{1-x}$,$Cr_x$)N coatings obtained from a $Ti_{0.70}Cr_{0.30}$ cathode, the chromium content gradually increases from x = 0.18 to x = 0.24. For a cathode with a lower chromium content, $Ti_{0.78}Cr_{0.22}$, the increase is less significant, from x = 0.11 to x = 0.13. In both cases, the chromium content in the coatings is lower than in the cathode, which is associated with the peculiarities of selective spraying of the growth surface [25]. It is known that under deposition conditions that ensure the formation of crystalline TiN, CrN coatings may have a less perfect crystalline structure [18], therefore, a higher chromium content in the cathode contributes to the amorphisation of Ti-Cr-N coatings. At the same time, the chromium content is not a determining factor in the formation of a nanocrystalline or amorphous-crystalline structure, since nitrogen pressure is also important. The formation of nitride coatings deposited from filtered highly ionised plasma occurs under conditions of intense ion bombardment of the surface. The composition, substructure, texture and residual stresses in the coatings of different systems are very sensitive to the substrate bias voltage and working gas pressure, which affect the energy of the bombarding particles of the metal plasma that form the coating [30–34]. With

increasing nitrogen pressure, the energy of the deposited particles decreases due to scattering on gas molecules, which leads to a weakening of the bombardment effect [35, 36].

The effect of Cr content on the hardness of Ti-Cr-N coatings is not clear-cut. It is known that the hardness of coatings depends on many factors, among which the decisive ones are not only the ratio of metal components, but also the nitrogen content, phase composition, substructure, defect density of the crystal structure, and the level of residual stresses [37]. The high microhardness of the obtained coatings $(Ti_{1-x},Cr_x)N$ (> 30 GPa) is mainly due to the nanostructure, and the additional increase in the hardness of coatings deposited using a cathode with a higher Cr content is associated with the effect of solid solution strengthening. When pressure changes, most of the characteristics of Ti-Cr-N coatings that affect hardness change. Fig. 2,b illustrates the effect of nitrogen pressure during deposition on the coatings hardness. When using a cathode with a lower chromium content, $Ti_{0.78}Cr_{0.22}$, an increase in pressure leads to a slight increase in the coatings hardness from 30.6 to 32.7 GPa, which can be attributed to an increase in the chromium content in the solid solution (see Fig. 2,a). For coatings deposited from a $Ti_{0.70}Cr_{0.30}$ cathode, with an increase in nitrogen pressure, despite the increase in the chromium content in the coatings, the hardness decreases from 45.6 to 35.8 GPa, most likely due to a decrease in stress levels during the transition from an amorphous-nanocrystalline to a nanocrystalline structure.

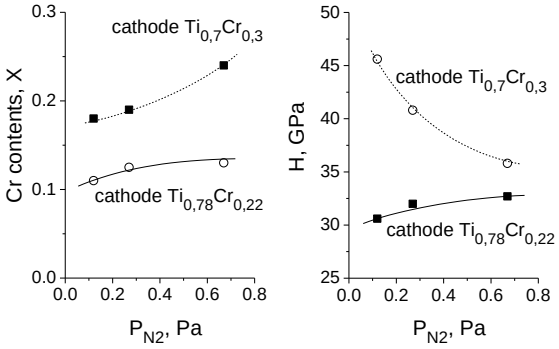


*a* *b*

*Fig. 2. Effect of nitrogen pressure during deposition on the chromium content (a) and hardness (b) of $(Ti_{1-x},Cr_x)N$ coatings deposited using cathodes of different compositions*

The results of tests for resistance to cavitation, friction and corrosion of specimens with coatings $(Ti_{1-x},Cr_x)N$ are shown in Figs. 3–5. Table 2 shows the hardness of the coatings, the average rate of cavitation and abrasive wear, and the potential at which pitting (local corrosion pits) begins to form. It can be seen that the protective characteristics of the coatings have certain differences.

Table 2

Results of coating tests $(Ti_{1-x},Cr_x)N$

| Specimen # | 1 | 2 | 3 | 4 | 5 | 6 |
|---|---|---|---|---|---|---|
| Coating composition | nc $(Ti_{0.89}Cr_{0.11})N$ | nc $(Ti_{0.87}Cr_{0.13})N$ | a/nc $(Ti_{0.82}Cr_{0.18})N$ | nc $(Ti_{0.76}Cr_{0.24})N$ | a/nc $(Ti_{0.81}Cr_{0.19})N$ | nc $(Ti_{0.75}Cr_{0.25})N$ |
| Hardness, GPa | 30.6 | 32.7 | 45.6 | 35.8 | 40.8 | 36.0 |
| Cavitation wear rate, μg/h | 83 | 123 | 300 | 167 | – | – |
| Abrasive wear rate, μg/h | 43 | 67 | 27 | 33 | 7 | – |
| Pitting potential, V | 0.72 | 0.89 | 0.50 | 0.75 | – | >1.4 |

Fig. 3 shows the kinetic curves of cavitation wear for specimens #1–4. Specimens with nanocrystalline coatings #1, 2, and 4 are characterised by fairly good wear resistance (with similar curves) and effectively resist cavitation effects for 3 h. During the first part of the test, 50…60% of the total weight loss of the coated specimens due to cavitation is observed, and then the wear rate decreases by 2–3 times. The average cavitation wear rate of nanocrystalline coatings is in the range of 83…167 μg/h. The best resistance is characterised by coating #1 nc $(Ti_{0.89}Cr_{0.11})N$ with a minimum chromium content, small nitride grains and a [110] texture. The specimen with coating #3 a/nc $(Ti_{0.82}Cr_{0.18})N$ coating, which has an amorphous-nanocrystalline structure, showed the worst protective properties with a consistently high wear rate of about 300 μg/h, which is 2–3 times higher than that of specimens with a nanocrystalline structure and quite close to the value for uncoated AISI 430 steel [38]. It should be noted that, as can be seen from Table 2 and Fig. 3, there is a clear correlation: an increase in hardness leads to a deterioration in cavitation resistance.

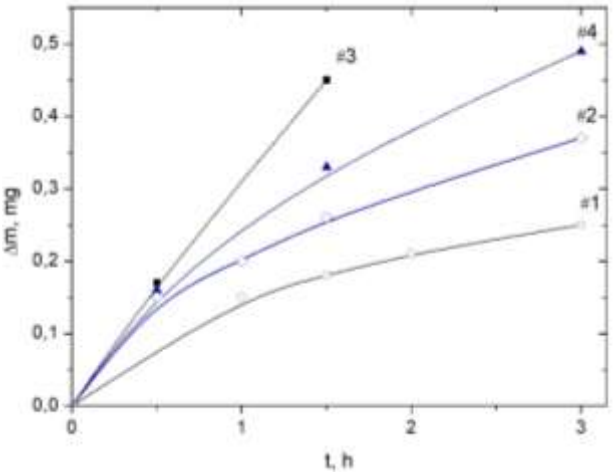


*Fig. 3. Kinetic curves of cavitation wear of specimens #1–4 with coatings $(Ti_{1-x},Cr_x)N$*

Fig. 4 shows the kinetic curves of abrasive wear of specimens #1–4. Data for the traditional TiN coating are given as well. It can be seen that all coatings $(Ti_{1-x},Cr_x)N$ are characterised by high wear resistance, much higher than that of the TiN coating. After just 0.5 h of testing, the TiN specimen had lost 0.12 mg in weight. As for the $(Ti_{1-x},Cr_x)N$ coatings, this figure is only 0.025…0.03 mg, and in further abrasive tests of coatings with a total duration of 1.5 h, the wear rate decreases significantly, similar to cavitation tests. The highest average abrasive wear rate of 67 μg/h was shown by a nanocrystalline coating with a relatively small amount of chromium #2 $nc(Ti_{0.87}Cr_{0.13})N$, which was characterised by the maximum size of solid solution crystallites and [111] texture. It can be seen that changing the texture to [110] or [100] and increasing the chromium content in the coating to 18…25 at.% contributes to improved wear resistance. No clear correlations between hardness and abrasion resistance were found, however, the hardest coating #3 $a/nc(Ti_{0.82}Cr_{0.18})N$ with an amorphous-nanocrystalline structure, which had the worst cavitation resistance, showed the lowest abrasive wear rate of 27 μg/h. The main destructive factor acting during abrasive wear is the cutting of material by a large number of micro-cutters, which are abrasive particles. Therefore, in the process of micro-cutting, the coating with the lowest hardness is more susceptible to material removal. In particular, the least resistant TiN coating had a hardness of only 27 GPa. Another factor that can reduce the abrasive resistance of traditional TiN coatings is deposition without the use of a plasma filter. It is known that coatings deposited by vacuum arc deposition from a direct (unfiltered) stream of metal plasma are characterised by a defective structure associated with the presence of cathode material macroparticles, which in the case of thin coatings can contribute to the formation of through pores and impair protective properties. In this work, coatings with a thickness of about 10 μm were investigated in order to minimise the influence of porosity and focus on the elemental composition and structure [38].

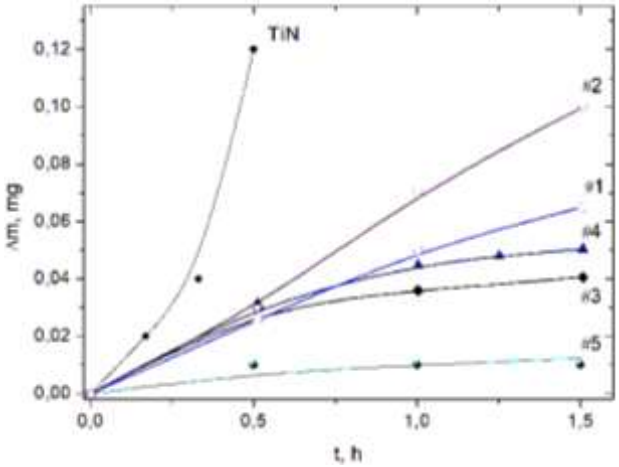


*Fig. 4. Kinetic curves of abrasive wear of specimens #1–4 with coatings $(Ti_{1-x},Cr_x)N$. For comparison, data are given for the traditional TiN coating and coating #5 $a/nc(Ti_{0.81}Cr_{0.19})N$, obtained by optimizing the deposition parameters*

Thus, coatings #3 and 4, obtained from a cathode with a high chromium content of $Ti_{0.7}Cr_{0.3}$ at two nitrogen pressures in the vacuum chamber of 0.12 and 0.67 Pa, respectively, showed the best abrasion resistance, with the amorphous-crystalline structure of coating #3 having advantages over the slightly higher chromium content in coating #4. Optimized coating #5 $a/nc(Ti_{0.81}Cr_{0.19})N$ was synthesized from the same cathode at an intermediate nitrogen pressure of 0.27 Pa, which allowed the amorphous-nanocrystalline structure to be preserved with an increased chromium content of 19 at.% and a reduced hardness value of 40.8 GPa compared to specimen #3. The results of abrasion tests of coating #5 (see Fig. 4 and Table 2) indicate extremely high wear resistance with an average abrasive wear rate of 7 μg/h, which is 3.8 times less than that of coating #3 $a/nc(Ti_{0.82}Cr_{0.18})N$ and 30 times less than that of TiN coating.

The results of corrosion tests of specimens in a 3% aqueous NaCl solution at room temperature are shown in Fig. 5. The anodic polarisation curves of specimens #1–4 as well as data for the AISI 430 steel substrate and traditional TiN coating are shown. The sharp rise in current on the j-E dependence for steel corresponds to the pitting reaction that occurs on the steel surface with the formation of soluble iron compounds [39, 40]. In relation to the substrate material, all coatings have a protective effect and shift the pitting potential to the positive range, but their anti-corrosion properties differ significantly. Both metals (Ti, Cr) that form the basis of the studied coatings are tend to passivation, which depends on the structure, roughness, stress and other characteristics of the coatings [41–44]. A comparison of the polarisation curves (see Fig. 5) shows that different processes occur in the studied specimens. The nature of the anode current growth can be associated with both the formation of oxides of different compositions (e.g., $Cr_2O_3$, $TiO_2$) and active dissolution (pitting corrosion).

It can be seen that deposition of a traditional TiN coating to the surface of AISI 430 steel leads to a decrease in anodic activity. The increase in potential in the first stage of testing does not cause significant changes in current. In the passive region, pitting begins at 0.3 V, and a further increase in voltage (> 0.55 V) leads to a sharp increase in anodic current, i.e., a transition from a passive state to an active dissolution mode is observed. The amorphous-nanocrystalline coating #3 $a/nc(Ti_{0.82}Cr_{0.18})N$ demonstrates slightly better behaviour, for which the pitting potential shifts to 0.5 V. The formation of a nanocrystalline structure contributes to a further increase in the corrosion resistance of $(Ti_{1-x},Cr_x)N$ coatings. Despite the maximum difference in chromium content between coatings #1 $nc(Ti_{0.89}Cr_{0.11})N$ and #4 $nc(Ti_{0.76}Cr_{0.24})N$ have fairly similar corrosion properties with pitting potentials of 0.72 and 0.75 V, respectively, after which the current density rapidly increases to 200 μA/cm$^2$. The nature of the anodic curve of specimen #2 $nc(Ti_{0.87}Cr_{0.13})N$ is fundamentally different. When the potential reaches 0.5 V, the anodic current begins to increase, but at 0.6 V growth stops and the current density of secondary passivation stabilizes at 38 μA/cm$^2$. The pitting potential shifts to 0.89 V, after

which the current again begins to increase, but not as fast as in other $(Ti_{1-x},Cr_x)N$ coatings. The current density is only 100 μA/cm$^2$ at a potential of 1.2 V.

Thus, coating #2, obtained from a cathode with a low chromium content of $Ti_{0.78}Cr_{0.22}$ at a nitrogen pressure of 0.67 Pa in a vacuum chamber, which showed the highest rate of abrasive wear, proved to be the most corrosion-resistant. Thanks to the optimization of the deposition parameters, coating #6 a/nc$(Ti_{0.75}Cr_{0.25})N$ was synthesised with a structure similar to specimen #2 with the highest chromium content of all the coatings studied, which showed the best corrosion resistance (see Fig. 4 and Table 2). The anodic curve of specimen #6 is similar to that of specimen #2, however, the low anodic current zone extends to 1 V, after which a slight increase begins until the passivation current density reaches 20 μA/cm$^2$, which is two times lower than in specimen #2. An increase in potential to 1.4 V does not lead to an increase in current and indicates high stability of the passive layer on the surface of specimen #6 and the absence of pitting damage in the studied potential range.

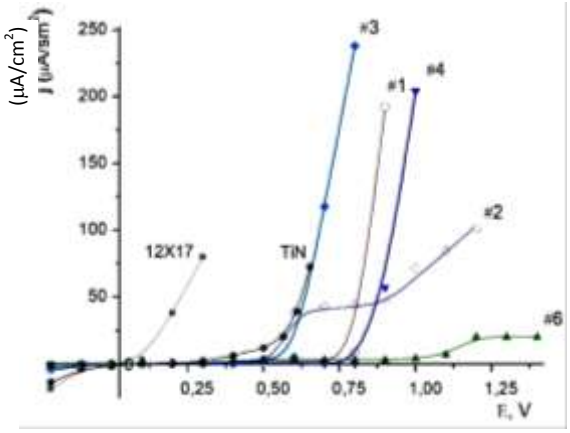


*Fig. 5. Anodic polarisation curves of specimens #1–4 with coatings $(Ti_{1-x},Cr_x)N$. For comparison, data are given for AISI 430 steel substrate, a traditional TiN coating and coating #6 nc$(Ti_{0.75}Cr_{0.25})N$, obtained by optimizing the deposition parameters*

The difference in the behaviour of the same coating in abrasive and cavitation tests is due to differences in wear mechanisms, which differ fundamentally both in the nature of the destructive forces and in the response of the coating to them. In addition, the mechanism of degradation of coated materials is complicated by the interference between the properties of the hard coating and the soft substrate. In [45], the desired resistance to cavitation and erosion of (Ti,Cr)N coatings was achieved through filtration, higher microhardness and good adhesion. An important feature of hard nanocrystalline coatings is that materials with high hardness H can differ significantly in terms of elastic modulus E. The combination of high hardness and low elastic modulus is considered optimal. The H/E ratio is often used to characterise the resistance of a material to elastic deformation and destruction [37]. However, the results obtained for TiN-based coatings (including those with the addition of Al, Si, Y, Zr, Nb and other elements), synthesized by vacuum arc deposition using filtered vacuum arc plasma, indicate that when predicting the wear resistance of coatings, it is necessary to take into account a complex of interrelated factors: hardness, H/E parameter, residual stress level, crystallite size, texture, surface roughness, and degree of columnar microstructure [33, 46, 47].

Cavitation degradation is mainly caused by impulse tangential stresses induced by hydrodynamic shocks, which is why cavitation erosion is fatigue-related. Increasing the strength and hardness of the tested material improves its cavitation resistance, while increasing its brittleness has the opposite effect. High bond strength and toughness, rather than simply hardness, are critical in cavitation wear. Another material parameter that significantly improves cavitation resistance is grain size reduction. Good adhesion as an essential parameter of coating resistance to cavitation erosion has also been noted [48]. In our experiments, high hardness did not contribute to improving the cavitation resistance of $(Ti_{1-x},Cr_x)N$ coatings. However, reducing the grain size in nanocrystalline coatings did have this effect. Partial amorphisation of the coating, which occurred with an increase in chromium content, had a negative effect on cavitation resistance.

During abrasion tests, wear occurs under the influence of constant mechanical contact with solid particles, therefore hardness and friction coefficient become more significant parameters determining wear resistance, but toughness cannot be neglected [49, 50]. We found that coatings $(Ti_{1-x},Cr_x)N$ with a high chromium content and high hardness >35 GPa show minimal abrasive wear, despite the difference in the amount of amorphous phase. Also, the negative effect on the abrasive resistance of the [111] texture was confirmed. It is known that the increased wear of coatings with a [111] texture is due to a high friction coefficient resulting from easy chipping of the material along the densely packed (111) planes of the FCC structure, which contributes to the formation of a large number of wear products that serve as abrasives [29]. At the same time, when testing $(Ti_{1-x},Cr_x)N$ coatings for corrosion resistance, the predominant [111] orientation showed advantages, as it hindered the diffusion of aggressive ions through the dense structure of the coating. It is believed that TiN coatings can provide higher hardness and friction resistance, while CrN coatings have higher viscosity and oxidation resistance. It is known that TiN-based coatings applied to stainless steel components corrode more due to galvanic bonding [19]. The addition of Cr to TiN improves corrosion resistance, but the amorphous phase in $(Ti_{1-x},Cr_x)N$ coatings does not resist corrosion well.

Several corrosion mechanisms exist through which a coating can lose its protective quality: local de-passivation by film-breakdown; local delamination of the coating, caused by inward diffusion of corrosive media followed by the formation of corrosion products at the coating-substrate interface; direct bypass of corrosive media at pin-holes. Macroparticles and growth defects stand at the center of the pitting mechanisms [51]. Since $(Ti_{1-x},Cr_x)N$ coatings were deposited from filtered plasma, the high corrosion

resistance of the applied coatings is largely due to the formation of a dense nanocrystalline structure without macroparticles and through-going columnar grains, which prevents the diffusion of the corrosive solution into the substrate.

## CONCLUSIONS

1. The cavitation, abrasion and corrosion resistance of vacuum arc coatings Ti-Cr-N were investigated. Nanostructured coatings with a thickness of 10 μm were deposited on AISI 430 steel substrates from filtered plasma flow using Ti-Cr cathodes containing 23 and 32 wt.% Cr at nitrogen pressures from 0.12 to 0.67 Pa. Nanocrystalline (nc) or amorphous-nanocrystalline (a/nc) coatings based on cubic solid solution $(Ti_{1-x},Cr_x)N$ with a chromium content from x = 0.11 to x = 0.25, an CSZ size in the range of 6…14 nm and different axial textures were tested. The coatings had a high hardness of 31…46 GPa, however, changes in the cathode composition and/or nitrogen pressure during deposition affected the chromium content in the coatings and their structure, which altered their protective properties. Nevertheless, all the coatings studied effectively protected the steel substrate during testing.

2. Nanocrystalline coatings with a low Cr content of 11…13 at.% and a hardness of 30…33 GPa showed the best resistance to cavitation wear. Applying such coatings to the surface of AISI 430 steel reduced the average cavitation wear rate by 2–3 times. The reduction in the size of the solid solution crystallites $(Ti_{1-x},Cr_x)N$ and the formation of the [110] texture contributed to the improvement of cavitation resistance. A clear correlation between the decrease in hardness and the improvement in cavitation resistance was found.

3. Coatings with a high Cr content of 18…24 at.% had the best abrasion resistance, with the amorphous-nanocrystalline structure of the a/nc$(Ti_{0.82}Cr_{0.18})N$ coating with high hardness of about 46 GPa had certain advantages, but it showed the worst results in cavitation and corrosion tests. Among the nanocrystalline structures, the nc$(Ti_{0.87}Cr_{0.13})N$ coating with the maximum size of solid solution crystallites, [111] texture, and hardness of 33 GPa, showed the highest level of abrasive wear. Changing the texture to [110] and increasing the chromium content in the coating contributed to improved abrasive resistance.

4. The results of corrosion resistance tests of specimens in a 3% aqueous NaCl solution showed that applying coatings to the surface of AISI 430 steel provides a significant protective effect and shifts the pitting potential to positive values due to passivation. The nc$(Ti_{0.87}Cr_{0.13})N$ coating with a [111] texture, which showed the worst resistance to abrasive wear, proved to be the most corrosion-resistant. The appearance of the anodic polarisation curve for this coating differs from other specimens and has a secondary passivated region. The pitting potential shifts to 0.89 V, after which the current begins to increase, but not as rapidly as in other $(Ti_{1-x},Cr_x)N$ coatings.

5. It has been shown that optimizing the deposition parameters during the synthesis of coatings with a high Cr content of around 25 at.% significantly improves the abrasion or corrosion resistance of coatings with amorphous-nanocrystalline and nanocrystalline structures, respectively. With regard to the comprehensive protection of steel products from cavitation, abrasion and corrosion, the use of nanocrystalline coatings appears to be the most appropriate.

## REFERENCES


1. A.I. Balitskii, A.M. Syrotyuk, V.O. Kolesnikov, V.O. Balitska, L.M. Ivaskevych, M.R. Havrilyuk. The Effect of Absorbed Hydrogen on the Rotors of Steel Machining Products During Powerful Turbo Aggregate Repairs // *Materials*. 2024, v. 17, p. 6257.

2. A.I. Balitskii, A.M. Syrotyuk, M.R. Havrilyuk, V.O. Balitska, V.O. Kolesnikov, L.M. Ivaskevych. Hydrogen Cooling of Turbo Aggregates and the Problem of Rotor Shafts Materials Degradation Evaluation // *Energies*. 2023, v. 16, p. 7851.

3. L.O. Slaston, M.G. Ishchenko, R.B. Sherfedinov, S.V. Alyokhina. Basic approaches to the choice of material for working blades of the last stages of the LPC of powerful steam turbines // *Problems of Atomic Science and Technology*. 2020, N 1(125), p. 215-219.

4. H.Yu. Rostova, G.D. Tolstolutska, R.L. Vasilenko, I.V. Kolodiy, V.I. Kovalenko, V.G. Marinin, M.A. Ti-khonovsky, O.S. Kuprin. Cavitation Wear of T91 Ferritic-Martensitic Steel // *Materials Science*. 2022, v. 58(3), p. 364-368.

5. W. Okuniewski, M. Walczak, M. Szala, D. Chocyk. Effect of surface modification by shot peening on cavitation erosion resistance of titanium alloy Ti-6Al-4V produced by DMLS method // *Engineering Failure Analysis*. 2025, v. 176, p. 109653.

6. I.O. Klimenko, V.G. Marinin, V.D. Ovcharenko, V.I. Kovalenko, A.S. Kuprin, O.M. Reshetnyak, V.A. Belous, H.Yu. Rostova. Resistance of titanium alloys to cavitation wear // *Problems of Atomic Science and Technology*. 2022, N 1(137), p. 130-135

7. H. Krechkovska, M. Hredil, O. Student, L. Svirska, S. Krechkovska, I. Tsybailo, P. Solovei. Peculiarities of fatigue fracture of high-alloyed heat-resistant steel after its operation in steam turbine rotor blades // *International Journal of Fatigue*. 2023, v. 167, Part B, p. 107341.

8. A. Krella. Resistance of PVD coatings to erosive and wear processes: A review // *Coatings*. 2020, v. 10(10), p. 921.

9. I.O. Klimenko, V.G. Marinin, V.A. Belous, N.A. Azarenkov, M.G. Ishchenko, V.S. Goltvyanytsya, A.S. Kuprin. Cavitation erosion resistance of vacuum-arc coatings based on TiN // *Problems of Atomic Science and Technology*. 2023, N 5, p. 126-136.

10. A. Krella. Cavitation erosion of monolayer PVD coatings – an influence of deposition technique on the degradation process // *Wear*. 2021, p. 478.

11. M. Szala, M. Walczak, K. Pasierbiewicz, M. Kami´nski. Cavitation Erosion and SlidingWear Mechanisms of AlTiN and TiAlN Films Deposited on Stainless Steel Substrate // *Coatings*. 2019, v. 9, p. 340.

12. J. Steller1, V. Safonov. New methodologies for assessing cavitation load and resistance of structural

materials and protective coatings in nuclear power industry. Part II. Polyfractional approach // *Problems of Atomic Science and Technology*. 2024, N 4, p. 126-131.

13. B. Warcholinski, A. Gilewicz, M. Tarnowska. The Surface Assessment and the Properties of Selected Multilayer Coatings // *Lubricants*. 2023, v. 11(9), p. 371.

14. J. Brezinova, J. Hasuľ, J. Brezina, P.O. Maruschak, J. Vinas. Determination of Tribological Properties of Multilayer Coatings Based on Nitrides // *Materials Science*. 2023, v. 58 (5), p. 629-635.

15. A. Do, D. Kim, H.J. Choi, S.W. Kim, S.Y. Lim, H.G. Lee, W.J. Kim. Improvement in the hydrothermal corrosion resistance of Ti-based nitride coatings by adding Cr for accident tolerant fuel cladding applications // *Journal of Nuclear Materials.* 2021, v. 549, p. 152903.

16. J.J. Ni, F. Liu, G. Yang, G.H. Lee, S.M. Chung, I.S. Lee, C. Chen. 3D-printed Ti6Al4V femoral component of knee: Improvements in wear and biological properties by AIP TiN and TiCrN coating // *Journal of Materials Research and Technology.* 2021, v. 14, p. 2322-2332.

17. J. Vetter, H.J. Scholl, O. Knotek. (TiCr)N coatings deposited by cathodic vacuum arc evaporation // *Surface and Coatings Technology*. 1995, v. 74-75, Part 1, p. 286-291.

18. S. Mohapatra, M-S. Oh. Evaluating the Tribological Properties and Residual Stress of TiCrN Thin Films Deposited by Cathodic-Arc Physical Vapor Deposition Technique // *Applied Sciences.* 2025, v. 15(5), p. 2466.

19. M.W. Reedy, T.J. Eden, J.K. Potter, D.E. Wolfe. Erosion performance and characterization of nanolayer (Ti,Cr)N hard coatings for gas turbine engine compressor blade applications // *Surface and Coatings Technology*. 2011, v. 206, p. 464-472.

20. D. Özkan, M.A. Yılmaz, C. Erdem, C. Türküz, E. Sulukan, M.B. Yağcı. Wear and Friction Behavior of CrTiN/TiCN and CrTiN/CrCN Multilayer Composite Coatings // *Ceramics International*. 2022, v. 48, p. 13732-13747.

21. M. Akbarzadeh, A. Shafyei, H.R. Salimijazi. Characterization of TiN, CrN and (Ti, Cr)N Coatings Deposited by Cathodic ARC Evaporation // *International Journal of Engineering.* 2014, v. 27, N 7, p. 1127-1132.

22. V. Vasyliev, A. Kalinichenko, F. Komarov, et al. Structure and Properties of Nitride Coatings Based on Ti and Cr Synthesized by PIII&D Technique // *Microstructure and Properties of Micro- and Nanoscale Materials, Films, and Coatings (NAP 2019)* / Pogrebnjak A., Bondar O. (eds.). Ch. 10, series Springer Proceedings in Physics. Springer Nature Singapore, 2020, p. 91-104.

23. V. Gorokhovsky, C. Bowman, D. VanVorous, J. Wallace. Deposition of various metal, ceramic, and cermet coatings by an industrial-scale large area filtered arc deposition process // *Journal of Vacuum Science and Technology A: Vacuum, Surfaces and Films*. 2009, v. 27(4), p. 1080-1095.

24. K. Valleti, C. Puneet, L. Rama Krishna, Shrikant V. Joshi. Studies on cathodic arc PVD grown TiCrN based erosion resistant thin films // *Journal of Vacuum Science and Technology A: Vacuum, Surfaces and Films.* 2016, v. 34(4), p. 041512.

25. Yu.A. Zadneprovskiy, V.A. Bilous, V.S. Goltvyanytsya, E.N. Reshetnyak, A.A. Komar. Mechanical characteristics and structure of vacuum arc Ti-Cr-N coatings // *Problems of Atomic Science and Technology*. 2025, N 2(156), p. 114-121.

26. Yu.A. Zadneprovskiy, V.A. Belous, I.S. Domnich, V.I. Kovalenko, H.Yu. Rostova, I.G. Tantsyura, G.N. Tolmachova, M.G. Ishchenko, A.S. Kuprin. Influence of the metal underlayer on the cavitation resistance of nitrided steel with $Mo_2N$ coating // *Problems of Atomic Science and Technology*, 2024, N 2, p. 101-106.

27. I.I. Aksenov, V.M. Khoroshikh. Filtering shields in vacuum-arc plasma sources // *Materials Science Forum*. 1998, v. 287-288, p. 283-286.

28. A. Anders. A structure zone diagram including plasma-based deposition and ion etching // *Thin Solid Films*. 2010, v. 518, p. 4087-4090.

29. S.S. Akkaya, V.V. Vasyliev, E.N. Reshetnyak, K. Ka-zmanlı, N. Solak, V.E. Strel'nitskij, M. Urgen. Structure and properties of TiN coatings produced with PIII&D technique using high efficiency rectilinear filter cathodic arc plasma // *Surface and Coatings Technology.* 2013, v. 236, p. 332-340.

30. V.V. Vasyliev, A.A. Luchaninov, E.N. Reshetnyak, et al. Structure and hardness of Ti-N and Ti-Si-N coatings deposited from the filtered vacuum-arc plasma // *Problems of Atomic Science and Technology.* 2009, N 2, p. 173-180.

31. V.A. Belous, A.S. Kuprin, S.N. Dub, et al. Structure and mechanical properties of Ti-Al-Si-N protective coatings deposited from separated plasma of a vacuum arc // *J. Superhard Mater*. 2013, v. 35, p. 20.

32. V.A. Belous, V.V. Vasilev, A.A. Luchaninov, et al. Hard coatings Ti-Al-N deposited from the filtered cathodic-arc plasma source // *Physical surface engineering*. 2009, v. 7, N 3, p. 216-222.

33. E.N. Reshetnyak, V.E. Strel'nitskij, V.V. Vasyliev, A.A. Luchaninov. Effect of pulsed substrate bias on the structure and properties of nitride coatings deposited by filtered cathodic arc plasma // *Problems of Atomic Science and Technology*. 2024, N 1, p. 176-188.

34. A. Kalinichenko, E. Reshetnyak, V. Strel'nitskij, G. Abadias. Role of nonlocal thermoelastic peaks in the stress and texture evolution of TiN coatings formed by plasma based ion implantation and deposition // *Surface and Coatings Technology.* 2020, v. 391, p. 125695.

35. I.I. Aksenov, A.A. Andreev, V.A. Belous, V.E. Strelnitskiy, V.M. Khorochikh. *Vacuum Arc: Plasma Sources, Deposition of Coatings, Surface Modification.* Kiev: "Naukova Dumka", 2012, p. 727.

36. A. Anders. *Cathodic Arcs From Fractal Spots to Energetic Condensation*. Springer Verlag New York, 2008. p. 540.

37. A. Gavaleiro, J.T. De. *Nano-structured Coatings*. New York: Springer, 2006, 648 p.

38. V.A. Belous, Yu. Zadneprovskiy, N. Lomino. Open pores and corrosion-cavitation resistance of vacuum-arc nitride coatings on titanium-base material with additives Si, Al and Y // *Proceedings of the XIV*

*International Conference on Problems of Corrosion and Anti-Corrosion Protection of Structural Materials, "Corrosion -2018"* (Ukraine, Lviv, June 5-7, 2018), p. 104-107.

39. V.V. Vasilyev, A.A. Luchaninov, V.E. Strel'nitskij, G.D. Tolstolutskaya, I.E. Kopanets, E.K. Sevidova, V.I. Kononenko. Corrosion resistant properties of AlN coating on bioengineering materials // *Problems of Atomic Science and Technology*. 2005, N 3, p. 167-170.

40. C.H. Hsu, C.K. Lin, K.H. Huang, K.L. Ou. Impro-vement on hardness and corrosion resistance of ferritic stainless steel via PVD-(Ti,Cr)N coatings // *Surface and Coatings Technology*. 2013, v. 231, p. 380-384.

41. H. Chen, Y. Zhao, Y. Liu, Y. Wu, & R. Hu. Characterisation and corrosion resistance of TiCrN composite coating on steel by physical vapour deposition // *Transactions of the Indian Institute of Metals.* 2016, v. 69(6), p. 1271-1277.

42. A. S. Dranenko, V.A. Lavrenko, V.N. Talash. Corrosion resistance of TiN films in 3 % NaCl solution // *Powder Metallurgy and Metal Ceramics.* 2013, v. 52, p. 223-227.

43. A.Y. Adesina, Z.M. Gasem, A. Madhan Kumar. Cor-rosion Resistance Behavior of Single-Layer Cathodic Arc PVD Nitride-Base Coatings in 1M HCl and 3.5 pct NaCl Solutions // *Metall. Mater. Trans.* 2017, B 48, p. 1321-1332.

44. H.A. Jehn. Improvement of the corrosion resistance of PVD hard coating–substrate systems // *Surface and Coatings Technology*. 2000, v. 125, issues 1-3, p. 212-217.

45. M.W. Reedy, T.J. Eden, J.K. Potter, D.E. Wolfe. Erosion performance and characterization of nanolayer (Ti,Cr)N hard coatings for gas turbine engine compressor blade applications // *Surface and Coatings Technology*. 2011, v. 206, issues 2-3, p. 464-472.

46. V.V. Vasyliev, V.S. Goltvyanytsya, S.K. Goltvyanytsya, A.A. Luchaninov, V.G. Marinin, E.N. Reshetnyak, V.E. Strel'nitskij, G.N. Tolmachova. Durability of the multicomponent nitride coatings based on TiN and (Ti,Al)N deposited by PIII&D method // *Problems of Atomic Science and Technology*. 2015, N 2, p. 130-138.

47. V. Belous, V. Vasyliev, A. Luchaninov, V. Marinin, E. Reshetnyak, V. Strel'nitskij, S. Goltvyanytsya, V. Goltvyanytsya. Cavitation and abrasion resistance of Ti-Al-Y-N coatings prepared by the PIII&D technique from filtered vacuum-arc plasma // *Surface and Coatings Technology*. 2013, v. 223, p. 68-74.

48. A. Krella. The influence of TiN coatings properties on cavitation erosion resistance // *Surface and Coatings Technology*. 2009, v. 204, issue 3, p. 263-270.

49. E. Lotfi-khojasteh, M. Sahebazamani, H. Elmkhah, M. Nouri, O. Imantalab, A. Fattah-alhosseini. A study of the electrochemical and tribological properties of TiN/CrN nano-layer coating deposited on carburized-H13 hot-work steel by Arc-PVD technique // *Journal of Asian Ceramic Societies*. 2021, v. 9, N 1, p. 270-282

50. Q. Zhou, Y. Ou, F. Li, C. Ou, W. Xue, B. Liao, Q. Hua, Y. Xu, J. Cao, G. Qu. Friction and Wear of Hard Yet Tough TiN Coatings Deposited Using High-Power Impulse Magnetron Sputtering // *Coatings.* 2024, v. 14, p. 598.

51. O.E. Hudak, A. Bahr, P. Kutrowatz, T. Wojcik, F. Bohrn, L. Solyom, R. Schuster, L. Shang, O. Hunold, P. Polcik, M. Heller, P. Felfer, G. Ball, H. Riedl. Pitting corrosion – Preferred chloride diffusion pathways in physical vapor deposited AlCrN coatings // *Corrosion Science*. 2023, v. 211, p. 110901.

*Article received 06.08.2025*

## ВПЛИВ СКЛАДУ ТА СТРУКТУРИ НА ЗАХИСНІ ВЛАСТИВОСТІ ВАКУУМНО-ДУГОВИХ ПОКРИТТІВ Ti-Cr-N

***Ю.А. Заднепровський, В.А. Білоус, О.М. Решетняк, В.С. Голтвяніца***

Досліджували кавітаційну, абразивну та корозійну стійкості вакуумно-дугових покриттів Ti-Cr-N. Наноструктурні покриття товщиною 10 мкм були нанесені на підкладки зі сталі AISI 430 із фільтрованого плазмового потоку з використанням Ti-Cr-катодів, що містили 23 та 32 мас.% Cr при тиску азоту від 0,12 до 0,67 Па. Випробувані нанокристалічні (nc) або аморфно-нанокристалічні (a/nc) покриття на основі кубічного твердого розчину $(Ti_{1-x},Cr_x)N$ з вмістом хрому від x = 0,11 до x = 0,25, розміром ОКР у межах 6…14 нм та різною текстурою аксіального типу. Покриття мали високу твердість (31…46 ГПа), однак зміна складу катода та/або тиску азоту при осадженні впливала на вміст хрому в покриттях та структуру, що змінювало їх захисні властивості. Проте усі досліджені покриття ефективно захищали сталеву підкладку при випробуваннях. Найкращу стійкість до кавітаційного зношування показали nc-покриття з низьким вмістом Cr – 11…13 ат.% і твердістю 30…33 ГПа. Зменшення розміру кристалітів твердого розчину $(Ti_{1-x},Cr_x)N$ та формування текстури [110] сприяло покращенню кавітаційної стійкості. Покриття з високим вмістом Cr (18…24 ат.%) мали найкращу абразивну стійкість, причому a/nc-структура з високою твердістю біля 46 ГПа мала певні переваги, однак вона показала найгірші результати при кавітаційних та корозійних випробуваннях. Покриття nc$(Ti_{0,87}Cr_{0,13})N$ з текстурою [111] та твердістю 33 ГПа виявилося найбільш корозійно-стійким, хоча мало найгіршу стійкість до абразивного зношування. Вигляд кривої анодної поляризації для цього покриття відрізняється від інших зразків і має область вторинної пасивації. Показано, що оптимізація параметрів осадження при синтезі покриттів з високим вмістом Cr (біля 25 ат.%) дозволяє додатково покращувати абразивну або корозійну стійкості покриттів з a/nc- та nc-структурами відповідно. Що стосується комплексного захисту поверхні сталевих виробів від впливу кавітації, абразиву та корозії найбільш доцільним представляється застосування нанокристалічних покриттів.